PHYSICAL REVIEW D **88,** 014501 (2013)

Coupled-channel scattering on a torus

Peng Guo,[1,*] Jozef J. Dudek,[1,2] Robert G. Edwards,[1] and Adam P. Szczepaniak[3,4]

[1]*Thomas Jefferson National Accelerator Facility, Newport News, Virginia 23606, USA*
[2]*Department of Physics, Old Dominion University, Norfolk, Virginia 23529, USA*
[3]*Physics Department, Indiana University, Bloomington, Indiana 47405, USA*
[4]*Center For Exploration of Energy and Matter, Indiana University, Bloomington, Indiana 47408, USA*

(Received 21 March 2013; published 1 July 2013)

Based on the Hamiltonian formalism approach, a generalized Lüscher's formula for two-particle scattering in both the elastic and coupled-channel cases in moving frames is derived from a relativistic Lippmann-Schwinger equation. Some strategies for extracting scattering amplitudes for a coupled-channel system from the discrete finite-volume spectrum are discussed and illustrated with a toy model of two-channel resonant scattering. This formalism will, in the near future, be used to extract information about hadron scattering from lattice quantum chromodynamics computations.

DOI: 10.1103/PhysRevD.88.014501 PACS numbers: 12.38.Gc, 11.80.Gw, 11.80.Jy, 13.75.Lb

I. INTRODUCTION

Hadron spectroscopy in lattice quantum chromodynamics (QCD) is entering a new era, in particular, recent developments in the application of variational methods [1–3] to large bases of hadron interpolating fields have made the extraction of the excited spectrum of hadronic states a realistic possibility (see e.g. [4–6]). Since excited hadrons appear as resonances in the continuous distribution of multihadron scattering states, to study hadron spectroscopy one requires evaluation of scattering amplitudes, but because lattice QCD is formulated in Euclidean space, we do not have direct access to these [7]. Fortunately, in a finite volume, interactions between particles as they evolve from the *in* to the *out* states lead to discrete changes in a free particle's energy that can be related to the scattering amplitude [8].

Various extensions to the framework derived by Lüscher in [8] have been proposed which allow for evaluation outside the center-of-mass frame [9–13], and to include the coupled-channel effects that can appear above the inelastic threshold [14–18]. The original approach and its extensions to describe the moving center-of-mass frame have been quite successfully used by the lattice community to extract elastic hadron-hadron scattering phase shifts [6,19–25].

In this work, we discuss a generalization of Lüscher's method for relativistic scattering in terms of a Hamiltonian where the specific interactions considered are based on a relativistic particle exchange model. We apply the technique to a two-channel system and a generalized Lüscher's equation for scattering in a moving frame is derived based on the relativistic Lippmann-Schwinger equation. The coupled-channel system has been considered previously [14,15,17,18], and our result agrees with these works. A novelty of the present work is to discuss practical strategies for extraction of scattering amplitude parameters from lattice simulations of a coupled-channel system. These strategies are demonstrated using an explicit toy model of resonant two-channel scattering.

The paper is organized as follows. A discussion of elastic scattering in a finite volume is given in Sec. II, with extension to the coupled-channel system in Sec. III. Strategies for extracting scattering amplitudes from measured discrete finite-volume spectra are presented in Sec. IV. The summary and outlook are given in Sec. V.

II. FINITE-VOLUME ELASTIC SCATTERING IN A HAMILTONIAN FRAMEWORK

In this section we present relativistic two-particle scattering on a torus using the Hamiltonian formalism developed in [26,27]. In particular we consider a complex scalar field Φ describing a charged boson $\phi^{\pm}$ of mass m, and its interactions with a neutral boson θ, which acts as a force carrier and is described by a real scalar field, Θ. We first derive the Lüscher formula describing the finite-volume spectrum of the asymptotic two-particle, $\phi^+\phi^-$ state,

$$\det\left[\delta_{JM,J'M'}\cot\delta_J(k) - \mathcal{M}^{(\mathbf{Q})}_{JM,J'M'}(k)\right] = 0,$$

where the volume and scattering-frame dependent matrix element $\mathcal{M}^{(\mathbf{Q})}_{JM,J'M'}$ is defined in Eqs. (B1) and (B3), and the center-of-mass frame scattering momentum k is related to the energy by $\sqrt{s/4-m^2}$. The model corresponds to a Lagrangian density,

$$\mathcal{L} = \partial_\mu\Phi^*\partial^\mu\Phi - m^2\Phi^*\Phi + \tfrac{1}{2}\partial_\mu\Theta\partial^\mu\Theta - \tfrac{1}{2}\mu^2\Theta^2 - g\Theta\Phi^*\Phi, \quad (1)$$

from which the Hamiltonian can be derived following the canonical procedure of instant-time quantization (see Appendix A) [28]. Taking matrix elements of the Hamiltonian in an infinite basis of Fock states spanned by any number of ϕ and θ bosons one can obtain a

*pguo@jlab.org

Schrödinger equation $\hat{H}|\Psi\rangle = E|\Psi\rangle$ for the eigenstates of the theory. Assuming $\mu \gg m$, in describing low-energy ϕ-boson scattering we can truncate the Fock space to include up to one θ boson in the intermediate state, which reduces the Schrödinger equation to

$$\begin{bmatrix} H_{22} & H_{23} \\ H_{32} & H_{33} \end{bmatrix} \begin{bmatrix} |\phi^+\phi^-\rangle \\ |\phi^+\phi^-\theta\rangle \end{bmatrix} = E \begin{bmatrix} |\phi^+\phi^-\rangle \\ |\phi^+\phi^-\theta\rangle \end{bmatrix}. \quad (2)$$

The three-particle sector can be formally eliminated, resulting in an effective two-body equation,

$$(E - H_{22})|\phi^+\phi^-\rangle = H_{23}\frac{1}{E - H_{33}}H_{32}|\phi^+\phi^-\rangle. \quad (3)$$

A. Two-particle scattering in an infinite volume

Before considering two-particle states on a torus, we will first review the scattering problem in infinite volume, with further details given in Appendix A. After eliminating the three-particle states $|\phi^+\phi^-\theta\rangle$ from the coupled system [cf. Eq. (2)] we are left with an equation for the center-of-mass frame momentum-space wave function, $\varphi_{JM}(\mathbf{q})$, which is a product of a radial wave function depending on the magnitude of the relative 3-momentum, $q = |\mathbf{q}|$, and the spherical harmonic of definite angular momentum, (J, M),

$$\varphi_{JM}(\mathbf{q}) = \frac{1}{\sqrt{s} - 2\sqrt{\mathbf{q}^2 + m^2}} \int \frac{d^3\mathbf{k}}{(2\pi)^3} V(\mathbf{q}, \mathbf{k})\varphi_{JM}(\mathbf{k}). \quad (4)$$

Here, $E = \sqrt{s}$ is the energy of the two-particle system in the center-of-mass frame. The nonlocal potential $V(\mathbf{q}, \mathbf{k})$ induced by θ exchange is given explicitly in Eq. (A1). Expressing this equation in coordinate space via a Fourier transform gives

$$\psi_{JM}(\mathbf{r}) = \int d^3\mathbf{r}' G_0(\mathbf{r} - \mathbf{r}'; \sqrt{s}) \int d^3\mathbf{z} \tilde{V}(\mathbf{r}', -\mathbf{z})\psi_{JM}(\mathbf{z}), \quad (5)$$

where the free Green's function is given by

$$G_0(\mathbf{r} - \mathbf{r}'; \sqrt{s}) = \int \frac{d^3\mathbf{q}}{(2\pi)^3} \frac{e^{i\mathbf{q}\cdot(\mathbf{r}-\mathbf{r}')}}{\sqrt{s} - 2\sqrt{\mathbf{q}^2 + m^2}}. \quad (6)$$

The wave function satisfies a relativistic Schrödinger equation,

$$\left(\sqrt{s} - 2\sqrt{-\nabla^2 + m^2}\right)\psi_{JM}(\mathbf{r}) = \int d^3\mathbf{z} \tilde{V}(\mathbf{r}, -\mathbf{z})\psi_{JM}(\mathbf{z}). \quad (7)$$

While Eq. (5) was derived in the context of a particular model, our subsequent derivation only requires the general form of the relativistic Lippmann-Schwinger equation. The asymptotic component of the two-body wave function relevant to scattering is given by the large distance behavior of the Green's function. Evaluating the integral in Eq. (6) (cf. Appendix A), we find

$$G_0(\mathbf{r}; \sqrt{s} = 2\sqrt{k^2 + m^2}) = -\frac{\sqrt{s}}{2}\frac{e^{ikr}}{4\pi r} - \frac{1}{r}\int_m^\infty \frac{\rho d\rho}{(2\pi)^2}\sqrt{\rho^2 - m^2}\frac{e^{-\rho r}}{k^2 + \rho^2}, \quad (8)$$

with the first term on the right-hand side dominating as $r \to \infty$. For a potential $\tilde{V}$ which falls at large separations, the solution to Eq. (7) outside the range of the interaction is given by

$$\psi_{JM}(\mathbf{r}) \to \frac{\sqrt{s}}{2m} i^J Y_{JM}(\hat{\mathbf{r}})[4\pi j_J(kr) + ikf_J(k)h_J^+(kr)], \quad (9)$$

where $f_J(k)$ is the partial wave scattering amplitude,

$$f_J(k) = -\frac{m}{i^J}\int d^3\mathbf{r}' d^3\mathbf{z} j_J(kr')Y^*_{JM}(\hat{\mathbf{r}}')\tilde{V}(\mathbf{r}', -\mathbf{z})\psi_{JM}(\mathbf{z}), \quad (10)$$

which up to the inelastic threshold can be parametrized in terms of a single real momentum-dependent parameter, the scattering phase shift, $\delta_J(k)$, as

$$f_J(k) = \frac{4\pi}{k} e^{i\delta_J} \sin\delta_J.$$

B. Two-particle scattering on a torus

Now we consider the theory in a cubic box of volume $V = L^3$, with periodic boundary conditions. In Eq. (5) we split the integral over $\mathbf{r}'$ into a sum of integrals over a set of boxes labeled by the integers $\mathbf{n}$ representing the location of one of its corners,

$$\psi^{(L)}_{JM}(\mathbf{r}) = \sum_{\mathbf{n}\in\mathbb{Z}^3} \int_{L^3} d^3\mathbf{r}' G_0(\mathbf{r} - \mathbf{r}' - \mathbf{n}L; \sqrt{s}) \times \int d^3\mathbf{z}' \tilde{V}(\mathbf{r}' + \mathbf{n}L, -\mathbf{z}' - \mathbf{n}L)\psi^{(L)}_{JM}(\mathbf{z}' + \mathbf{n}L). \quad (11)$$

In general we can make the wave functions periodic up to a phase,

$$\psi^{(L)}_{JM}(\mathbf{z} + \mathbf{n}L) = e^{i\mathbf{Q}\cdot\mathbf{n}L}\psi^{(L)}_{JM}(\mathbf{z}),$$

where the Bloch wave vector $\mathbf{Q}$ is related to the total momentum of the two-particle system [9] by $\mathbf{P} = 2\gamma\mathbf{Q}$. $\gamma = \sqrt{s + \mathbf{P}^2}/\sqrt{s}$ is the Lorentz contraction factor that reduces the effective size of the box in the direction parallel to $\mathbf{P}$. Using the periodicity of the potential, $\tilde{V}(\mathbf{r}' + \mathbf{n}L, -\mathbf{z}' - \mathbf{n}L) = \tilde{V}(\mathbf{r}', -\mathbf{z}')$, and the boundary condition on the wave function, we have

$$\psi_{JM}^{(L,\mathbf{Q})}(\mathbf{r}) = \int_{L^3} d^3\mathbf{r}' G_{\mathbf{Q}}(\mathbf{r}-\mathbf{r}';\sqrt{s}) \times \int d^3\mathbf{z}\tilde{V}(\mathbf{r}',-\mathbf{z})\psi_{JM}^{(L,\mathbf{Q})}(\mathbf{z}),$$

which is analogous to the infinite-volume equation, but with the Green's function given by

$$G_{\mathbf{Q}}(\mathbf{r}-\mathbf{r}';\sqrt{s}) = \sum_{\mathbf{n}\in\mathbb{Z}^3} G_0(\mathbf{r}-\mathbf{r}'-\mathbf{n}L;\sqrt{s})e^{i\mathbf{Q}\cdot\mathbf{n}L}.$$

Using the Poisson summation formula, $(2\pi)^{-3}\sum_{\mathbf{n}\in\mathbb{Z}^3} e^{i\mathbf{Q}\cdot\mathbf{n}L} = L^{-3}\sum_{\mathbf{n}\in\mathbb{Z}^3}\delta(\mathbf{Q}+\frac{2\pi}{L}\mathbf{n})$, we obtain

$$G_{\mathbf{Q}}(\mathbf{r}-\mathbf{r}';\sqrt{s}) = \frac{1}{L^3}\sum_{\mathbf{q}\in P_{\mathbf{Q}}} \frac{e^{i\mathbf{q}\cdot(\mathbf{r}-\mathbf{r}')}}{\sqrt{s}-2\sqrt{\mathbf{q}^2+m^2}} \to \frac{\sqrt{s}}{2}\frac{1}{L^3}\sum_{\mathbf{q}\in P_{\mathbf{Q}}} \frac{e^{i\mathbf{q}\cdot(\mathbf{r}-\mathbf{r}')}}{k^2-\mathbf{q}^2},$$

where $P_{\mathbf{Q}} = \{\mathbf{q}\in\mathbb{R}^3 | \mathbf{q} = \frac{2\pi}{L}\mathbf{n}+\mathbf{Q}, \text{ for } \mathbf{n}\in\mathbb{Z}^3\}$, and where we have retained only the leading term in the limit $L \gg |\mathbf{r}-\mathbf{r}'| \gg m^{-1}$. Finally, expanding Eq. (11) for $r \gg r'$ and using the definition of the scattering amplitude, Eq. (10), we can express the wave function as

$$\psi_{JM}^{(L,\mathbf{Q})}(\mathbf{r}) \to \frac{\sqrt{s}}{2m}(-k)i^J f_J(k)\sum_{J'M'} Y_{J'M'}(\hat{\mathbf{r}}) \times [\delta_{JM,J'M'} n_{J'}(kr) - \mathcal{M}^{(\mathbf{Q})}_{JM,J'M'}(k) j_{J'}(kr)]. \tag{12}$$

The residual sum over all angular momenta reflects the broken rotational invariance induced by the finite cubic volume, with the volume-dependent matrix elements $\mathcal{M}$ given in Appendix B. In the infinite-volume case, the most general solution of the relativistic Schrödinger equation, Eq. (7), outside the range of the potential is $\sum_{JM} c_{JM}\psi_{JM}(\mathbf{r})$ for $\psi_{JM}(\mathbf{r})$ given by Eq. (9). Correspondingly in finite volume, the most general solution is given by $\sum_{JM} c_{JM}\psi_{JM}^{(L,\mathbf{Q})}(\mathbf{r})$ for $\psi_{JM}^{(L,\mathbf{Q})}(\mathbf{r})$ given by Eq. (12). Matching the two wave functions at a fixed r, larger than the range of the interaction, we obtain

$$\sum_{JM} c_{JM} Y_{JM}(\hat{\mathbf{r}}) i^J [4\pi j_J(kr) + ikf_J(kr)h_J^+(kr)] = -\sum_{JM,J'M'} c_{JM} i^J k f_J(k) Y_{J'M'}(\hat{\mathbf{r}}) \times [\delta_{JM,J'M'} n_{J'}(kr) - \mathcal{M}^{(\mathbf{Q})}_{JM,J'M'}(k) j_{J'}(kr)],$$

which has a nontrivial, $c_{JM} \neq 0$, solution provided

$$\det[\delta_{JM,J'M'}\cot\delta_J(k) - \mathcal{M}^{(\mathbf{Q})}_{JM,J'M'}(k)] = 0. \tag{13}$$

This condition expresses the relationship between the asymptotic behavior of the two-particle wave function on a torus expressed through the matrix elements $\mathcal{M}^{(\mathbf{Q})}_{JM,J'M'}$, and the effect of the interaction on the wave function determined by the phase shifts, δ_J. In practice for a given set of elastic phase shifts, $\delta_J(k)$, it determines a discrete spectrum of states in a finite volume.

The analysis presented here can be generalized to an arbitrarily shaped box. In general the three edges of the box are spanned by three arbitrary vectors $\mathbf{L}_{1,2,3}$. The volume of the cube L^3 is replaced by $(\mathbf{L}_1\times\mathbf{L}_2)\cdot\mathbf{L}_3$ and the vector $\mathbf{n}L$ by $\sum_{i=1,2,3} n_i\mathbf{L}_i$, $n_i\in\mathbb{Z}$. Finally the momentum $\mathbf{q} = 2\pi\mathbf{n}/L, \mathbf{n}\in\mathbb{Z}^3$ is replaced by generalized momentum $2\pi\sum_{i=1,2,3} n_i(\mathbf{L}_j\times\mathbf{L}_k)/|(\mathbf{L}_1\times\mathbf{L}_2)\cdot\mathbf{L}_3|$, $n_i\in\mathbb{Z}$, where the indices (i,j,k) follow the cyclic permutation. Such a generalization has to be considered when using the moving center-of-mass frame since the symmetric shape of a cubic box in the rest frame is deformed due to Lorentz contraction [9]. In this case if $\mathbf{P} = 2\pi\mathbf{d}/L, \mathbf{d}\in\mathbb{Z}^3$ is the center-of-mass momentum, the volume of the box becomes γL^3, and the vectors $\mathbf{n}L$ and $2\pi\mathbf{n}/L$ are replaced by $\gamma\mathbf{n}L$ and $2\pi\gamma^{-1}\mathbf{n}/L$, respectively (using the notation defined in [9]). With these substitutions and the relation $\mathbf{P} = 2\gamma\mathbf{Q}$, our definition of the matrix elements $\mathcal{M}^{(\mathbf{Q})}_{JM,J'M'}$ becomes identical to the matrix elements $M^{\mathbf{d}}_{lm,l'm'}$ in Eq. (89) of [9].

Typically, as discussed in [8], for the low-energy region that we are interested in, higher partial waves become progressively smaller and can be ignored so that the partial wave basis can be truncated at a certain maximal angular momentum $J_{\max}$. For a finite volume with cubic boundaries, the continuous rotation symmetry is reduced to the little group of allowed cubic rotations that leave the center-of-mass momentum invariant—the matrices in Eq. (13) become block diagonal if subduced according to the irreducible representations of these little groups. Details of subduction in general moving frames can be found in [29].

III. COUPLED-CHANNEL SCATTERING IN FINITE VOLUME

We extend the model of the previous section to include additional two-particle asymptotic states by adding another species of charged bosons, $\sigma^{\pm}$, which also couple to the force carrier θ into the Lagrangian. We can obtain coupled equations for the two-particle states, $|\phi^+\phi^-\rangle$ and $|\sigma^+\sigma^-\rangle$, by eliminating states featuring three or more particles and obtain a two-channel Schrödinger equation,

$$|\phi^+\phi^-\rangle = \frac{1}{E-H_\phi^{(0)}}[V_{\phi\phi}|\phi^+\phi^-\rangle + V_{\phi\sigma}|\sigma^+\sigma^-\rangle],$$
$$|\sigma^+\sigma^-\rangle = \frac{1}{E-H_\sigma^{(0)}}[V_{\sigma\phi}|\phi^+\phi^-\rangle + V_{\sigma\sigma}|\sigma^+\sigma^-\rangle], \tag{14}$$

where $H_\phi^{(0)}$, $H_\sigma^{(0)}$ are the one-particle operators and $V_{\phi\phi}$, $V_{\phi\sigma}$, $V_{\sigma\phi}$, $V_{\sigma\sigma}$ are effective interactions (two-body operators) generated by the reduction to the two-particle subspace. From Eq. (14), for the channel wave functions, $\psi_{JM}^{\alpha=\phi,\sigma}(\mathbf{r}) \equiv \langle\mathbf{r}|\alpha, JM\rangle$, we obtain

$$\psi^{\alpha}_{JM}(\mathbf{r}) = \int d^3\mathbf{r}' G^{\alpha}_0(\mathbf{r}-\mathbf{r}';\sqrt{s}) \times \sum_{\beta}\int d^3\mathbf{z}\tilde{V}_{\alpha\beta}(\mathbf{r}',-\mathbf{z})\psi^{\beta}_{JM}(\mathbf{z}).$$

The coupled-channel scattering amplitudes can be defined by

$$f^{\alpha\beta}_J(s) = -\frac{m_\alpha}{i^J}\int d^3\mathbf{r}' d^3\mathbf{z} j_J(k_\alpha r') Y^*_{JM}(\hat{\mathbf{r}}')\tilde{V}_{\alpha\beta}(\mathbf{r}',-\mathbf{z})\psi^{\beta}_{JM}(\mathbf{z}), \quad (15)$$

where $k_\alpha = \sqrt{s/4 - m_\alpha^2}$ is the magnitude of the relative momentum in the center-of-mass frame of the two particles in channel α. By analogy to the single-channel case, the asymptotic wave function in channel α is given by

$$\psi^{\alpha}_{JM}(\mathbf{r}) \to \frac{\sqrt{s}}{2m_\alpha} Y_{JM}(\hat{\mathbf{r}}) i^J \times \left[4\pi j_J(k_\alpha r) + i k_\alpha h^+_J(k_\alpha r)\sum_\beta f^{\alpha\beta}_J(s)\right]. \quad (16)$$

Extending the one-channel analysis of the asymptotic states in finite volume to the two-channel system, one obtains

$$\psi^{\alpha(L,\mathbf{Q})}_{JM}(\mathbf{r}) \to \frac{\sqrt{s}}{2m_\alpha}(-k_\alpha) i^J \sum_{J'M'} Y_{J'M'}(\hat{\mathbf{r}})\left[\sum_\beta f^{\alpha\beta}_J(s)\right] \times [\delta_{JM,J'M'} n_{J'}(k_\alpha r) - \mathcal{M}^{(\mathbf{Q})}_{JM,J'M'}(k_\alpha) j_{J'}(k_\alpha r)]. \quad (17)$$

Matching the wave functions in finite volume, Eq. (17), to the wave functions in infinite volume, Eq. (16), we get a determinant condition

$$\det\left[\delta_{JM,J'M'}\delta_{\alpha,\beta}\frac{4\pi}{k_\alpha}\frac{1}{f^{\alpha\alpha}_J} + [i\delta_{JM,J'M'} - \mathcal{M}^{(\mathbf{Q})}_{JM,J'M'}(k_\alpha)]\frac{f^{\alpha\beta}_J}{f^{\alpha\alpha}_J}\right] = 0. \quad (18)$$

The derivation logically extends to any number of scattering channels. Expressing the scattering amplitudes using t-matrix elements, $t^{(J)}_{\alpha\beta}(s) \equiv \frac{\sqrt{s}}{8\pi} f^{\alpha\beta}_J(s)$, and introducing the phase space for channel α by $\rho_\alpha(s) = \frac{2k_\alpha}{\sqrt{s}}$, we can write the condition as

$$0 = \det[\delta_{JM,J'M'}\delta_{\alpha,\beta} + i\rho_\alpha(s) t^{(J)}_{\alpha\beta}(s)(\delta_{JM,J'M'} + i\mathcal{M}^{(\mathbf{Q})}_{JM,J'M'}(k_\alpha))], \quad (19)$$

or, alternatively in a form which expresses the effect of unitarity more directly as

$$0 = \det[\delta_{JM,J'M'}([t^{(J)}(s)]^{-1}_{\alpha\beta} + i\rho_\alpha(s)\delta_{\alpha,\beta}) - \delta_{\alpha,\beta}\rho_\alpha(s)\mathcal{M}^{(\mathbf{Q})}_{JM,J'M'}(k_\alpha)]. \quad (20)$$

The multichannel unitarity condition can be expressed as $\mathrm{Im}[t^{(J)}(s)]^{-1}_{\alpha\beta} = -\delta_{\alpha\beta}\rho_\alpha(s)\Theta(s - s^{(\alpha)}_{\mathrm{thr}})$, and thus, since $\rho_\alpha(s)$ becomes pure imaginary below threshold, the first term in Eq. (20) is always real.

The form presented in Eq. (19) can be shown to be equivalent to that presented in [17,18]. Their expressions include an additional phase of $i^{J-J'}$ in front of $\mathcal{M}$, but the effect of this phase is always canceled in the determinant.

Reflecting the remaining symmetry of a cube in flight, there is in fact one determinant condition for each irreducible representation (irrep) of the symmetry group. As presented in [6,29], these conditions can be obtained by subduction, the result being conditions

$$0 = \det[\delta_{JJ'}\delta_{nn'}([t^{(J)}(s)]^{-1}_{\alpha\beta} + i\rho_\alpha(s)\delta_{\alpha,\beta}) - \delta_{\alpha,\beta}\rho_\alpha(s)\mathcal{M}^{(\mathbf{Q},\Lambda)}_{Jn,J'n'}(k_\alpha)], \quad (21)$$

where the Λ-irrep subduced $\mathcal{M}^{(\mathbf{Q},\Lambda)}_{Jn,J'n'}(k_\alpha)$ is as defined in Eq. (28) of [6]. The angular-momentum space is defined by the various embeddings, n, of spin J into the irrep Λ. If the subduction conventions in [6] are followed, for unitary t matrices, the conditions are purely real at all real energies.

The two-channel scattering matrix $f^{\alpha\beta}$ can be conventionally parametrized in terms of two scattering phase shifts, $\delta^\alpha_J(s)$ ($\alpha = \phi, \sigma$), and an inelasticity $\eta_J(s)$ representing the fraction of flux exchanged between the two channels,

$$f^{\alpha\alpha}_J(s) = \frac{4\pi}{k_\alpha}\cdot\frac{\eta_J e^{2i\delta^\alpha_J} - 1}{2i}; \qquad f^{\alpha\beta}_J(s) = \frac{4\pi}{\sqrt{k_\alpha k_\beta}}\cdot\frac{\sqrt{1-\eta_J^2}e^{i(\delta^\alpha_J + \delta^\beta_J)}}{2}, \quad (22)$$

so that the determinant condition can be written

$$\det\begin{bmatrix} \delta_{JM,J'M'}\cot\Delta^\phi_J - \mathcal{M}^{(\mathbf{Q})}_{JM,J'M'}(k_\phi) & \sqrt{\frac{k_\phi}{k_\sigma}}[i\delta_{JM,J'M'} - \mathcal{M}^{(\mathbf{Q})}_{JM,J'M'}(k_\phi)]\frac{\sqrt{1-\eta_J^2}e^{i\Delta^\sigma_J}}{2\eta_J\sin\Delta^\phi_J} \\ \sqrt{\frac{k_\sigma}{k_\phi}}[i\delta_{JM,J'M'} - \mathcal{M}^{(\mathbf{Q})}_{JM,J'M'}(k_\sigma)]\frac{\sqrt{1-\eta_J^2}e^{i\Delta^\phi_J}}{2\eta_J\sin\Delta^\sigma_J} & \delta_{JM,J'M'}\cot\Delta^\sigma_J - \mathcal{M}^{(\mathbf{Q})}_{JM,J'M'}(k_\sigma) \end{bmatrix} = 0, \quad (23)$$

where $\Delta^\alpha_J(s) \equiv \delta^\alpha_J(s) - \frac{i}{2}\log\eta_J(s)$. One can show that this result is equivalent to Eq. (4.14) in [14].

The determinant conditions presented above for coupled-channels scattering provide only one equation, at each finite-volume energy, for many unknowns. At low energies we may be justified in only considering the effect of the lowest contributing partial wave, but even then there are multiple unknowns. For example in the case of two-channel scattering in S wave we require three parameters to describe the t matrix at each energy which might be the two phase shifts and inelasticity, δ_0^ϕ, δ_0^σ, η_0. Hence additional constraints need to be imposed to obtain a unique solution. As an example, in [15] a unitarized chiral perturbation theory was used to constrain amplitude parameters at low energies. In the next section we explore some strategies for extraction of the scattering amplitude from finite-volume spectra in the context of an analytical parametrization of the amplitude.

It is worth noting here that in a finite volume, kinematically closed channels can play a role in determining the spectrum. Examining Eq. (19), we see that the behavior of $\mathcal{M}^{(\mathbf{Q})}_{JM,J'M'}(k)$, analytically continued below threshold (to imaginary k) must be considered. These matrix elements decay rapidly below threshold, such that the effect of a kinematically closed channel on the finite-volume spectrum is only felt in a limited energy region below the kinematic threshold. For example if $k = i\kappa$,

$$\mathcal{M}^{(\mathbf{Q})}_{00,00}(i\kappa) = i - \frac{i}{\kappa}\sum_{\substack{\mathbf{n}\in\mathbb{Z}^3\\ \mathbf{n}\neq 0}} \frac{e^{-\kappa|\gamma\mathbf{n}L|}}{|\gamma\mathbf{n}L|} e^{i\mathbf{Q}\cdot\gamma\mathbf{n}L},$$

so that far below threshold, or in very large volume, $\mathcal{M} \to i$, and thus in Eq. (19), the effect of this channel is removed. However this closed channel will have an effect in a region just below the threshold, for $\gamma\kappa \lesssim L^{-1}$. Hence we are required in practice to analytically continue scattering amplitudes below thresholds in order to determine the finite-volume spectrum. An example of this is presented in [30] for the case of S-wave $\pi\Sigma$, $\overline{K}N$ scattering.

IV. A TOY MODEL OF RESONANT COUPLED-CHANNEL SCATTERING IN FINITE VOLUME

In order to explore possible strategies for extracting coupled-channel scattering amplitudes from the discrete finite-volume spectra emerging from lattice QCD computations, we consider a simple model of two-channel S-wave scattering. The model is based on resonance-dominated scattering and satisfies multichannel unitarity and the analytical properties required of partial wave amplitudes. With an explicit model for scattering amplitudes we can solve Eq. (19) to obtain finite-volume spectra of states as a function of the volume ($V = L^3$) and total momentum of the center-of-mass $\mathbf{P} = 2\pi\mathbf{d}/L$, $\mathbf{d} \in \mathbb{Z}^3$ ($\mathbf{P} = 2\gamma\mathbf{Q}$). We then use this spectrum as pseudodata representing a hypothetical lattice QCD simulation and attempt to reproduce the input model.

A. Analytic model of two-channel scattering

We consider a model in which a single S-wave resonance coupled to both scattering channels interferes with a nonresonant background. The two-channel scattering amplitude is parametrized in terms of a K matrix,

$$K_{\alpha\beta}(s) = \frac{g_\alpha g_\beta}{M^2 - s} + \gamma^{(0)}_{\alpha\beta} + \gamma^{(1)}_{\alpha\beta} s + \cdots, \qquad (24)$$

which is related to the t matrix by

$$[t^{-1}(s)]_{\alpha\beta} = [K^{-1}(s)]_{\alpha\beta} + \delta_{\alpha\beta} I_\alpha(s),$$

and to the scattering amplitude defined in Eq. (15) by $t_J^{\alpha\beta}(s) = \sqrt{s} f_J^{\alpha\beta}(s)/8\pi$ with ($\alpha = \phi,\ \sigma$). Here $I_\alpha(s)$ is the Chew-Mandelstam form [31],

$$I_\alpha(s) = I_\alpha(0) - \frac{s}{\pi}\int_{4m_\alpha^2}^{\infty} ds' \sqrt{1 - \frac{4m_\alpha^2}{s'}} \frac{1}{(s' - s)s'},$$

whose imaginary part above threshold, i.e. for $s > 4m_\alpha^2$, is the negative of the phase space, $\mathrm{Im}[I_\alpha(s)] = -\rho_\alpha(s)$. This form ensures the unitarity of the amplitude and provides a smooth transition across the kinematic threshold. We have opted to subtract the integral once, and it is convenient to choose $I_\alpha(0)$ such that $\mathrm{Re}I_\alpha(M^2) = 0$ so that we have an amplitude which for real s near M^2 is close to the Breit-Wigner form with mass M. The t matrix thus constructed is an analytical function in the complex s plane with the discontinuity across the right-hand cut determined by unitarity.

With the following choice of parameters,

$$m_\phi = 0.2\,\mathrm{GeV}, \quad m_\sigma = 0.4\,\mathrm{GeV}, \quad M = 1.1\,\mathrm{GeV},$$
$$g_\phi = 0.35\,\mathrm{GeV}, \quad g_\sigma = 0.2\,\mathrm{GeV}, \quad \gamma^{(n)}_{\phi\phi} = \gamma^{(n)}_{\phi\sigma} = 0,$$
$$\gamma^{(0)}_{\sigma\sigma} = 0.7, \quad \gamma^{(1)}_{\sigma\sigma} = 0.7\,\mathrm{GeV}^{-2}, \quad \gamma^{(n>1)}_{\sigma\sigma} = 0,$$

we obtain the phase shifts and inelasticity shown in Fig. 1. The parameters have been chosen in such a way that there is a narrow resonance near $\sqrt{s} = 1.1$ GeV. It is usual to analyze scattering in terms of the most relevant

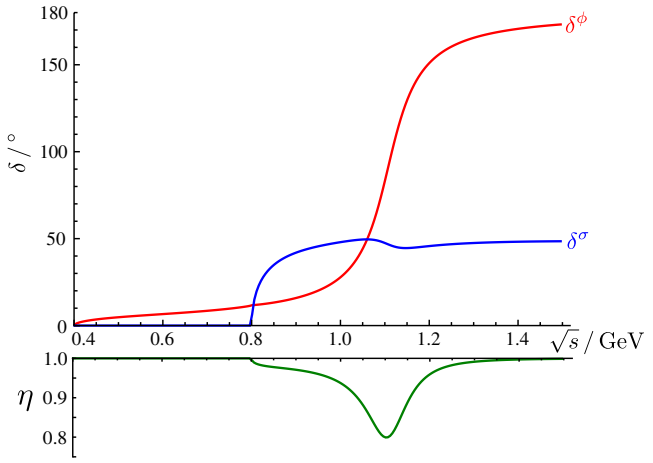

FIG. 1 (color online). Phase shifts and inelasticity for the model defined in the text.

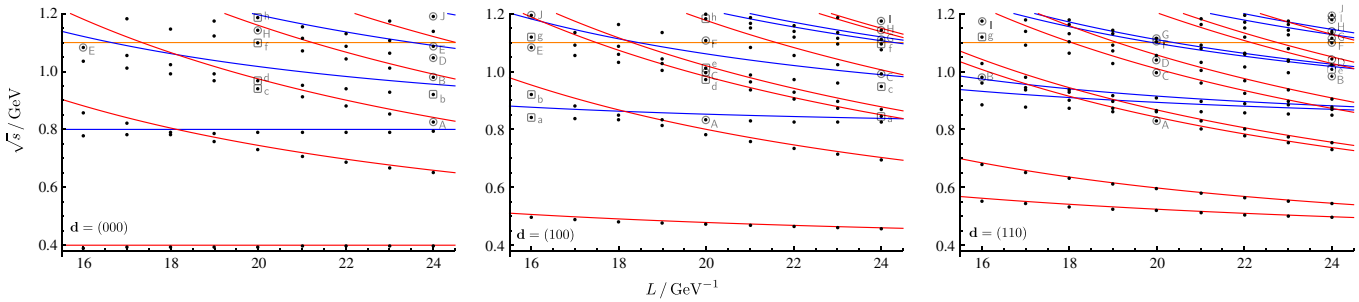

FIG. 2 (color online). Finite-volume spectra for the K-matrix model described in Sec. IV A. Black dots indicate the spectrum obtained by solving Eq. (19). Red and blue curves represent the energy of a noninteracting pair of mesons ($\alpha = \phi, \sigma$) $[(\sqrt{m_\alpha^2 + \mathbf{k}_1^2} + \sqrt{m_\alpha^2 + \mathbf{k}_2^2})^2 - \mathbf{P}^2]^{1/2}$, $\mathbf{k}_1 + \mathbf{k}_2 = \mathbf{P}$, and $\mathbf{k} = \frac{2\pi}{L}\mathbf{n}$, $\mathbf{n} \in \mathbb{Z}^3$. The points labeled by letters are used as described in the text.

singularities of the t matrix on the nearby unphysical sheets. Poles on unphysical sheets are often identified with hadron resonances. In this case the four sheets (sheet I is the physical sheet) can be defined by

$$[t_{\text{sheet}}^{-1}(s)]_{\alpha\beta} = \begin{cases} [t_{\text{I}}^{-1}(s)]_{\alpha\beta} & \text{sheet I} \\ [t_{\text{I}}^{-1}(s)]_{\alpha\beta} + 2i\sqrt{1 - \frac{4m_\phi^2}{s}}\delta_{\alpha\phi} & \text{sheet II} \\ [t_{\text{I}}^{-1}(s)]_{\alpha\beta} + 2i\sqrt{1 - \frac{4m_\alpha^2}{s}}\delta_{\alpha\beta} & \text{sheet III} \\ [t_{\text{I}}^{-1}(s)]_{\alpha\beta} + 2i\sqrt{1 - \frac{4m_\sigma^2}{s}}\delta_{\alpha\sigma} & \text{sheet IV} \end{cases}.$$

The model amplitude has a single pole on the lower half-plane[1] of each of sheets II and III, with the t matrix in the neighborhood of the pole at s_0 behaving like

$$[t_{\text{sheet}}(s \to s_0)]_{\alpha\beta} \to \frac{c_\alpha c_\beta}{s_0 - s},$$

with

$$\begin{aligned} \sqrt{s_0} &= (1.1067 - \tfrac{i}{2}0.0961)\ \text{GeV}, \\ c_\phi &= (0.3585\ \text{GeV})e^{-i0.0023\pi}, \\ c_\sigma &= (0.1367\ \text{GeV})e^{-i0.237\pi} \end{aligned}$$

on sheet II and

$$\begin{aligned} \sqrt{s_0} &= (1.1088 - \tfrac{i}{2}0.1195)\ \text{GeV}, \\ c_\phi &= (0.3573\ \text{GeV})e^{+i0.0026\pi}, \\ c_\sigma &= (0.1391\ \text{GeV})e^{+i0.297\pi} \end{aligned}$$

on sheet III. Our aim is to use the finite-volume spectrum determined on a set of volumes and total momenta, $\mathbf{P}$, to reproduce the pole positions of this scattering amplitude.

B. Finite-volume spectrum

The finite-volume spectrum corresponding to the model defined in the previous section can be obtained by solving Eq. (23) [or equivalently Eq. (19)], where for $E = \sqrt{s} < 2m_\sigma$ we require the analytic continuation of t-matrix elements featuring channel σ. Assuming that partial waves higher than S wave are negligible reduces Eq. (23) for $E > 2m_\sigma$ to

$$\begin{aligned} 0 &= \Omega(\delta^\phi(E), \delta^\sigma(E), \eta(E); L, \mathbf{d}; E) \\ &= \eta[\mathcal{M}_\phi - \mathcal{M}_\sigma]\sin(\delta^\phi - \delta^\sigma) \\ &\quad + [\mathcal{M}_\phi + \mathcal{M}_\sigma]\sin(\delta^\phi + \delta^\sigma) \\ &\quad - \eta[1 + \mathcal{M}_\phi\mathcal{M}_\sigma]\cos(\delta^\phi - \delta^\sigma) \\ &\quad - [1 - \mathcal{M}_\phi\mathcal{M}_\sigma]\cos(\delta^\phi + \delta^\sigma), \end{aligned} \tag{25}$$

where $\mathcal{M}_\phi \equiv \mathcal{M}^{(\mathbf{Q})}_{J=0M=0,J'=0M'=0}(k_\phi)$ with a similar expression for $\mathcal{M}_\sigma$. $\mathbf{Q}$ is a function of $\mathbf{d}$, L, E as discussed in Sec. II B. In Fig. 2 we show the finite-volume spectrum[2] obtained by solving the determinant condition as a function of the volume in a region $L = 16$–24 GeV^{-1} (or $L = 3.2$–4.7 fm).

C. "Pointwise" estimation of scattering from finite-volume spectrum

In the region below $2m_\sigma$ the $\phi\phi$ scattering is elastic and it is tempting to use Eq. (13), completely ignoring the existence of the kinematically closed $\sigma\sigma$ channel. Doing so leads to the points shown in pink in Fig. 3 which successfully reproduce the input model except in a region just below the threshold. As previously discussed, in a finite volume the effect of a closed channel can be felt within a limited energy region immediately below the threshold. With this in mind, we must be careful not to use the simple elastic relation, Eq. (13), close to a threshold.

One approach to determining the phase shifts and inelasticities at discrete values of energy above $2m_\sigma$ is to locate multiple energy levels (in different volumes and/or different $\mathbf{d}$) that appear at approximately the same energy. As an example consider the three levels labeled A in Fig. 2

[1] And a conjugate pole on the upper half-plane.

[2] This would be the spectrum in irrep A_1 [6].

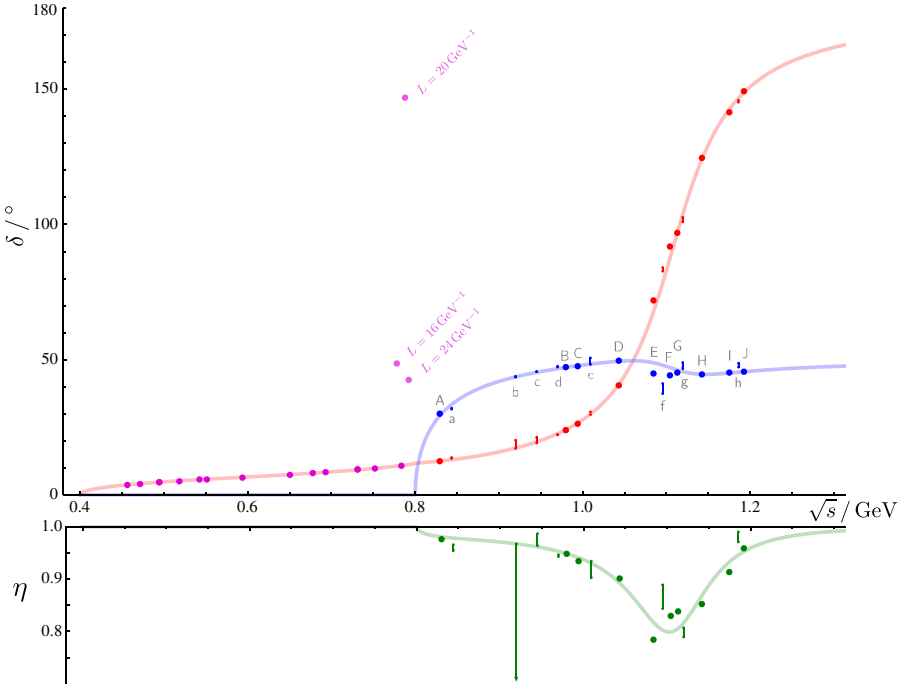

FIG. 3 (color online). "Pointwise" determination of the phase shifts and inelasticity. δ^ϕ points below the opening of the $\sigma\sigma$ threshold (in pink) are determined by solving the elastic relation, Eq. (13), ignoring the effect of the closed channel. The badly discrepant points just below the threshold are all within a momentum scale of $1/L$ of the threshold where the finite-volume effect of the closed channel should not be neglected. Energies A–J are determined from constrained three-level analysis and energies a–h by interpolation in δ^ϕ from two-level analysis. The light-colored curves show the exact input model.

which all lie within 3 MeV of $\sqrt{s_A} = 830$ MeV. For the three levels we can build three independent copies of Eq. (23) which each feature approximately the same values of $\delta^\phi(s_A)$, $\delta^\sigma(s_A)$, $\eta(s_A)$, which can be determined by solving the set of simultaneous equations. Since the energies are not *exactly* degenerate, there need not be an exact solution to the equations and hence we seek to find the solution which minimizes

$$\sum_{E(L,\mathbf{d})} |\Omega(\delta^\phi, \delta^\sigma, \eta; L, \mathbf{d}; E)|^2,$$

with Ω defined in Eq. (25) and where the sum is over the three energy levels. For the levels A, the obtained solution, as shown in Fig. 3, is within 3% of the exact value of $\delta^\phi(s_A)$, $\delta^\sigma(s_A)$, $\eta(s_A)$. We emphasize that this procedure is not guaranteed to successfully reproduce the true scattering amplitudes—the $\mathcal{M}$ matrices can in some circumstances vary rather rapidly over a narrow energy region.

Within the energy region considered, $E = 0.8$–1.2 GeV, considering only three volumes, $L = 16, 20, 24$ GeV^{-1}, and three sets of center-of-mass momentum, $\mathbf{d} = (000)$, (100), (110), we can isolate a number of such sets. These sets of three near-degenerate energy levels are labeled A–J in Fig. 2. In Fig. 3 the labels are shown on the plot of δ^ϕ with the corresponding solutions for δ^σ and η marked by solid dots.

With these points alone, in Fig. 3 we see strong hints of a signal for resonant behavior in the δ^ϕ phase shift. While obviously reasonably successful, this approach does not make optimal use of the finite-volume spectral information, by failing to use any energy level which does not have two near-degenerate partners. To use somewhat more of the discrete levels we might consider building a system of *two* instances of Eq. (23) with one parameter from the set δ^ϕ, δ^σ, η estimated using interpolation between already determined values. For example consider the two levels near 1.009 GeV labeled e in Fig. 2. Linear interpolation between the energies of the C and D points in Fig. 3 gives $\delta^\phi(1.009\text{ GeV}) = 30.7°$. Using this value and minimizing with respect to δ^σ, η at the energy corresponding to point e we obtain $\delta^\sigma = 50.6°$, $\eta = 0.903$. A spline interpolation using all the points A–J yields $\delta^\phi(1.009\text{ GeV}) = 29.6°$ which results in $\delta^\sigma = 48.1°$, $\eta = 0.934$ at the point e. In Fig. 3 we show the results for sets of two degenerate levels labeled a–h from Fig. 2. In each case the range shown indicates limiting values obtained using two methods of interpolation. Even though in some cases there is a considerable sensitivity to the interpolation method, overall the points are in reasonable agreement with the model input (solid light-colored curves).

D. Parametrized estimation of scattering from finite-volume spectrum

The previously discussed "pointwise" strategy, while having the advantage of being largely model independent,

is reliant upon there being multiple energy levels which, through accident or design, are close to degenerate. Since it would be unusual to engineer lattice volumes purely for this purpose, and unusual in contemporary calculations to have such a high density of determined energy levels, it is appropriate to consider alternative methods of analysis. One such approach that makes full use of all determined levels, and which may require far fewer levels to be determined, involves parametrizing the scattering amplitude and performing a minimization to get the best description of the determined finite-volume spectrum by varying the parameters. In the current toy model, even limited "pointwise" analysis would suggest that the phase δ^{ϕ} is rapidly rising and would indicate that a resonance could be present. In practical calculations (e.g. [4,32]), the presence of a sharp meson resonance can also be indicated by large overlap onto fermion bilinear operators. By including a pole (as well as polynomial behavior) in a K-matrix parametrization we are likely to get rapid convergence to a solution with a pole in the t matrix corresponding to the resonance.

We will take this opportunity to make the toy model a slightly more realistic simulation of an actual lattice QCD calculation by introducing statistical uncertainty on the energy level values. In recent work [6,22,32], the Hadron Spectrum Collaboration has obtained statistical errors on excited levels as small as 0.3% and we will assume that this remains practical. For each energy level below 1.2 GeV on a single volume $L = 16\ \mathrm{GeV}^{-1} \sim 3.2$ fm with $\mathbf{d} = (000)$, (100), (110), we randomly generate an ensemble by drawing from a distribution whose mean is the exact value given in Fig. 2 and whose variance is chosen such that the ensemble has variance on the mean of 0.3% of the mean value. The resulting spectrum is shown in Fig. 4.

Parametrizing according to a form like that given in Eq. (24), we can minimize a function,

$$\chi^2(\{a_i\}) = \sum_{E_{\mathrm{n}}(L,\mathbf{d})} \frac{[E_{\mathrm{n}}(L,\mathbf{d}) - E_{\mathrm{n}}^{\mathrm{det}}(L,\mathbf{d};\{a_i\})]^2}{\sigma(E_{\mathrm{n}}(L,\mathbf{d}))^2},$$

[where E^{det} are the solutions of Eq. (19)], by varying the parameters of the K-matrix parametrization, $\{a_i\} = \{M, g_{\phi}, g_{\sigma}, \gamma^{(n)} \ldots\}$. In practical lattice QCD calculations, the χ^2 can be trivially redefined to deal with correlated data by replacing the inverse diagonal variance $(1/\sigma^2)$ by the inverse of the data covariance matrix.

In Fig. 5 we show the parametrized phase shifts and inelasticity obtained using five model parametrizations:

(i) A: "exact model," which uses a first order polynomial in s to describe the nonpole contribution to the K matrix with $\gamma^{(0,1)}_{\phi\phi} = \gamma^{(0,1)}_{\phi\sigma} \equiv 0$ (five parameters),

(ii) B: "relaxed model," with a first order polynomial in all channels i.e. all $\gamma^{(0,1)}$ free (nine parameters),

(iii) C: "tight model," with zeroth order of polynomials in all channels i.e. $\gamma^{(1)} = 0$ (six parameters),

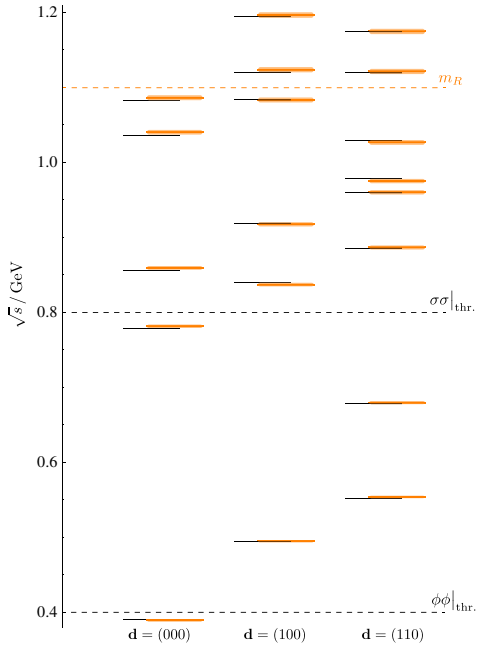

FIG. 4 (color online). $L = 16\ \mathrm{GeV}^{-1}$. Orange rectangles: finite-volume spectra with 0.3% noise. Black lines: exact finite-volume spectrum given in Fig. 2. Also shown the position of the thresholds and the K-matrix pole mass.

(iv) D: "loose model," with second order of polynomials in all channels i.e. $\gamma^{(0,1,2)}$ free (12 parameters),

(v) E: "two pole model," with no polynomials, but with a second K-matrix pole with independent variable couplings (six parameters).

As one would expect, within statistical uncertainty, parametrization A reproduces the input model. Parametrization B, which is more flexible, also reproduces the input quite well over the energy region where data are given, albeit with a larger statistical uncertainty, but begins to show signs of deviation from the original K matrix in the energy range outside of the fit region. Parametrization C does not have sufficient flexibility to describe the complete energy dependence—while it does correctly reproduce the resonance shape in δ^{ϕ} and the presence of a dip in η, the precise energy dependence of η is not correct and it fails to describe δ^{σ} at high energies, away from the energy region where the pole dominates. Parametrization D introduces too much parameter-space freedom for the limited set of data points available. As such we see rapid energy variation that is not really required and a large degree of statistical uncertainty. Parametrization E shows that a precise knowledge of the form of the "background" is not required to reproduce the energy dependence in a limited region—a second K-matrix pole (at higher energy) is able to mock up the polynomial behavior away from the resonance pole quite well.

All the above parametrizations include at least one pole in the K matrix—a feature that is not strictly necessary to

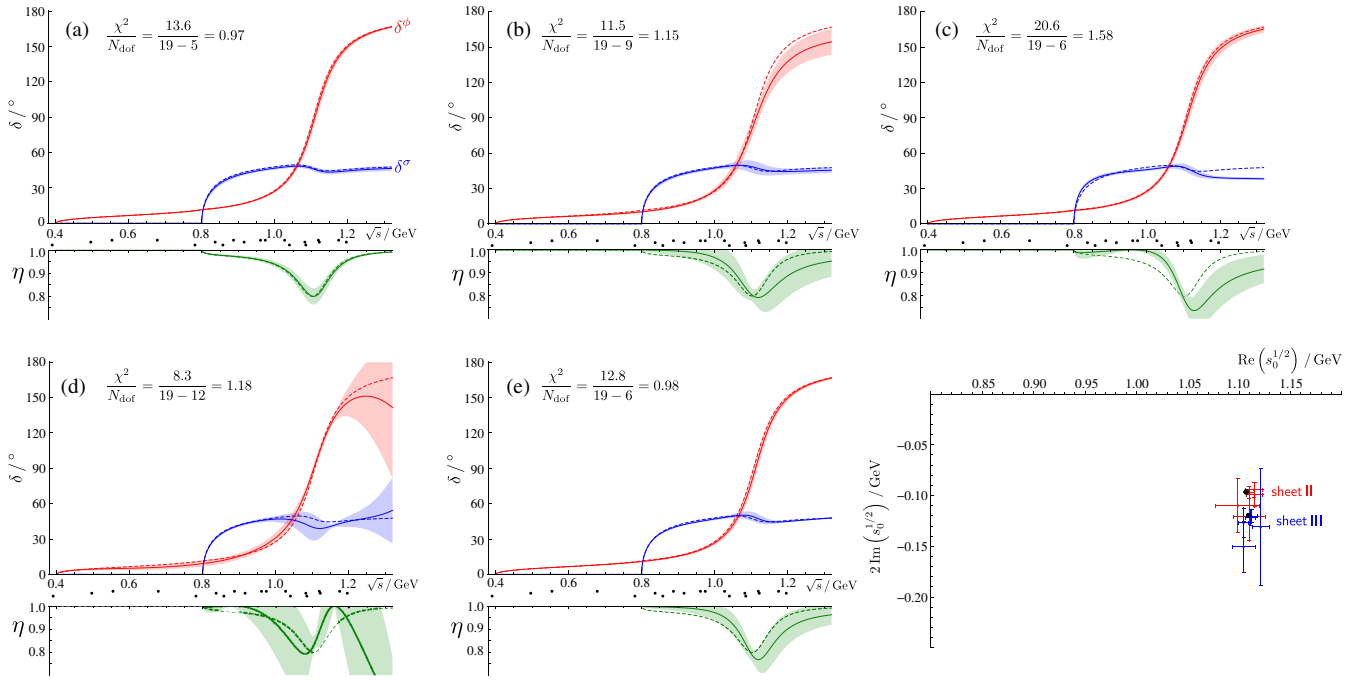

FIG. 5 (color online). Best-fit phase shifts and inelasticity for the parametrizations A–E as described in the text. Solid curves with error bands show the minimized solutions with the dashed curves showing the exact input. Black dots under the energy scale show the positions of the discrete energy levels used in the minimization. Bottom-right panel shows the determined position of a t-matrix pole on the unphysical sheets II (red) and III (blue) for the five parametrizations along with the exact input positions (black dots).

generate a pole in the t matrix. In principle, polynomial behavior in K can give rise to poles in t. In the current case, probably due to the fact that the resonance is rather narrow, fits to the finite-volume spectrum that included only a polynomial in K and no poles did not give rise to descriptions with reasonable χ^2. Going to a higher order polynomial introduces too much parameter-space freedom and fits typically fail to converge. The rapid rise in $\delta_\phi(s)$ suggested by even limited "pointwise" analysis of the spectrum, and the low χ^2's associated with the fits A–E, suggest that a parametrization that generates a pole in $t(s)$ close to the real axis is required to describe the finite-volume spectrum.

Our principal interest lies in identifying resonances as poles in the complex-s plane—analytically continuing the fitted model amplitudes we find that all five have single poles on sheets II and III whose locations are in a rather good agreement with the input pole position (see Fig. 5). The residues at the pole agree similarly. The statistical precision of the pole position determination typically decreases as we introduce more parameters into the model. The pleasing observation here is that in order to determine the position of a sharp resonance we do not need to have precise knowledge of the form of the energy dependence of the "background."

In summary, the "pointwise" strategy may provide a less model-dependent approach for extracting phase shifts and inelasticities, however, this method is limited by the number of points for which accidental degeneracies appear. Parametrizing the scattering amplitude allows us to make use of all measured energy levels, however we need to find suitable parametrizations. One strategy is to explore the "pointwise" approach to find a crude guide to the energy dependence and then build parametrizations which are able to reproduce the obtained form. The parametrizations, which should respect certain constraints applicable to scattering amplitudes, can be made progressively more sophisticated in an effort to reduce the overall χ^2—in this sense the approach is not dissimilar to what is done with real experimental data.

V. SUMMARY

Using the Hamlitonian formalism applied to a model of interacting relativistic fields, we derived a generalized Lüscher's formula [8,9,14,15] for two-particle scattering, in both the single- and coupled-channel systems, in moving frames.

Our results were consistent with the ones obtained previously in [8,9,14,15]. In the coupled-channel case we were challenged by the fact that, even for dominance of a single partial wave, the system was underconstrained for determination of multiple-channel phase shifts and inelasticities from a single determined finite-volume energy level. Using a toy model of two-channel S-wave scattering we demonstrated that it is possible to determine this information if multiple energy levels are determined.

Two possible strategies for extracting information from discrete spectra of a coupled-channel system were

discussed, one approach utilized the near degeneracy of energy levels in different volumes and total momenta of system, and another fits the discrete spectra by parametrizing the scattering amplitudes with certain numbers of parameters. These strategies may be useful for the analysis of future lattice QCD data. In particular, the coupled-channel analysis has to be considered for the strongly coupled systems, for instance, $\pi\pi$, $K\bar{K}$, and $\eta\eta$ system in S wave.

ACKNOWLEDGMENTS

We thank D. B. Renner and M. R. Pennington for useful discussions, and our colleagues within the Hadron Spectrum Collaboration for their continued assistance. P. G., R. G. E., and J. J. D. acknowledge support from U.S. Department of Energy Contract No. DE-AC05-06OR23177, under which Jefferson Science Associates, LLC manages and operates Jefferson Laboratory. J. J. D. also acknowledges the support of the U.S. Department of Energy Early Career Award Contract No. DE-SC0006765. A. P. S. acknowledges the support of the U.S. Department of Energy grant under Contract No. DE-FG0287ER40365.

APPENDIX A: RELATIVISTIC LIPPMANN-SCHWINGER EQUATION FROM HAMILTONIAN FORMALISM

Following the method presented in [26,27], we treat the relativistic dynamics of particle scattering in the Hamiltonian formalism approach. We start from the covariant Lagrangian in Eq. (1) and choose to quantize the field operators in the instant form [28]; the construction of generators of the Poincaré group can be done in a standard way in quantum field theory. In principle, one needs to solve eigenstate equations $\hat{H}|\Psi\rangle = E|\Psi\rangle$ on an instant quantization plane, where $|\Psi\rangle$ denotes the Poincaré covariant state vector spanning the complete Fock space. We truncate the Fock space up to three-body states, assuming that this is sufficient to describe low-energy physics. Thus, the eigenstate equations reduce to a matrix equation given in Eq. (2). Eliminating the three-body sector, we end up with the relativistic Schrödinger-like equation for a two-body system given in Eq. (3). For simplicity, we have assumed that the two charged scalars scattering have equal mass, however, the conclusion of this work can be generalized to the nonequal masses case as well (cf. [33,34]).

We choose the center-of-mass frame of the many-body system to construct multiple-particle states $|JM\rangle$ having total spin J and spin projection M. The two-particle state $|\phi^+\phi^-\rangle$ in the center-of-mass frame is given by

$$|\phi^+\phi^-; JM\rangle = 2\sqrt{s}\int \frac{d^3\mathbf{p}_1}{(2\pi)^3 2E_{p_1}} \frac{d^3\mathbf{p}_2}{(2\pi)^3 2E_{p_2}} \delta^3(\mathbf{p}_1 + \mathbf{p}_2) \times (2\pi)^3 \varphi^{(2)}_{JM}(\mathbf{p}_1, \mathbf{p}_2) a^\dagger_{\mathbf{p}_1} b^\dagger_{\mathbf{p}_2}|0\rangle,$$

where $\mathbf{p}_i$ is the momentum of the ith particle and $\sqrt{s}$ is the invariant mass of the two-particle system. $\varphi^{(2)}_{JM}(\mathbf{p}_1, \mathbf{p}_2)$ is the wave function of the two-particle system describing the momentum distribution of the two particles.

Similarly, the three-particle state $|\phi^+\phi^-\theta\rangle$ is given by

$$|\phi^+\phi^-\theta; JM\rangle = 2\sqrt{s}\int \frac{d^3\mathbf{p}_1}{(2\pi)^3 2E_{p_1}} \frac{d^3\mathbf{p}_2}{(2\pi)^3 2E_{p_2}} \frac{d^3\mathbf{p}_3}{(2\pi)^3 2E_{p_3}} \times (2\pi)^3 \delta^3(\mathbf{p}_1 + \mathbf{p}_2 + \mathbf{p}_3) \times \varphi^{(3)}_{JM}(\mathbf{p}_1, \mathbf{p}_2, \mathbf{p}_3) a^\dagger_{\mathbf{p}_1} b^\dagger_{\mathbf{p}_2} d^\dagger_{\mathbf{p}_3}|0\rangle,$$

where $\varphi^{(3)}_{JM}(\mathbf{p}_1, \mathbf{p}_2, \mathbf{p}_3)$ is the wave function of the three-particle system. The wave functions are normalized so that the normalization of states is $\langle JM|JM\rangle = 2\sqrt{s}(2\pi)^3\delta^3(\mathbf{0})$.

It is straightforward to evaluate the matrix elements of the eigenstate equations Eq. (2) and to get coupled equations for the wave functions

$$\varphi^{(2)}_{JM}(\mathbf{q}) = \frac{g}{\sqrt{s} - 2\sqrt{\mathbf{q}^2 + m^2}} \int \frac{d^3\mathbf{k}'}{(2\pi)^3 2\sqrt{\mathbf{k}'^2 + \mu^2}} \left[\frac{\varphi^{(3)}_{JM}(\mathbf{q} + \frac{1}{2}\mathbf{k}', \mathbf{k}')}{2\sqrt{(\mathbf{q} + \mathbf{k}')^2 + m^2}} + \frac{\varphi^{(3)}_{JM}(\mathbf{q} - \frac{1}{2}\mathbf{k}', \mathbf{k}')}{2\sqrt{(\mathbf{q} - \mathbf{k}')^2 + m^2}} \right],$$

$$\varphi^{(3)}_{JM}(\mathbf{q}, \mathbf{k}) = g \frac{\frac{1}{2\sqrt{(\frac{1}{2}\mathbf{k} - \mathbf{q})^2 + m^2}} \varphi^{(2)}_{JM}(\mathbf{q} - \frac{1}{2}\mathbf{k}) + \frac{1}{2\sqrt{(\frac{1}{2}\mathbf{k} + \mathbf{q})^2 + m^2}} \varphi^{(2)}_{JM}(\mathbf{q} + \frac{1}{2}\mathbf{k})}{\sqrt{s} - \sqrt{(\frac{1}{2}\mathbf{k} + \mathbf{q})^2 + m^2} - \sqrt{(\frac{1}{2}\mathbf{k} - \mathbf{q})^2 + m^2} - \sqrt{\mathbf{k}^2 + \mu^2}},$$

where we have used a shorthand notation for wave functions $\varphi^{(2)}_{JM}(\mathbf{q})$ and $\varphi^{(3)}_{JM}(\mathbf{q}, \mathbf{k})$, with arguments of relative momenta defined by $\mathbf{q} = \frac{1}{2}(\mathbf{p}_1 - \mathbf{p}_2)$, $\mathbf{k} = -\mathbf{p}_3$. Eliminating the three-body wave function, we get a relativistic equation for the two-particle state $|\phi^+\phi^-\rangle$ with an effective nonlocal potential generated from the neutral scalar exchange between two charged scalars

$$\varphi^{(2)}_{JM}(\mathbf{q}) = \frac{1}{\sqrt{s} - 2\sqrt{\mathbf{q}^2 + m^2}} \int \frac{d^3\mathbf{k}}{(2\pi)^3} V(\mathbf{q}, \mathbf{k}) \varphi^{(2)}_{JM}(\mathbf{k}),$$

with

$$V(\mathbf{q},\mathbf{k}) = \frac{g^2}{4}\frac{1}{1-\Sigma(\mathbf{q})}\frac{1}{(\mathbf{k}^2+m^2)}\frac{1}{\sqrt{(\mathbf{k}-\mathbf{q})^2+\mu^2}}\frac{1}{\sqrt{s}-\sqrt{\mathbf{k}^2+m^2}-\sqrt{\mathbf{q}^2+m^2}-\sqrt{(\mathbf{k}-\mathbf{q})^2+\mu^2}}, \quad \text{(A1)}$$

where the self-energy contribution is

$$\Sigma(\mathbf{q}) = \frac{1}{\sqrt{s}-2\sqrt{\mathbf{q}^2+m^2}}\frac{g^2}{4}\int\frac{d^3\mathbf{k}'}{(2\pi)^3}\frac{1}{\sqrt{s}-\sqrt{\mathbf{k}'^2+m^2}-\sqrt{\mathbf{q}^2+m^2}-\sqrt{(\mathbf{k}'-\mathbf{q})^2+\mu^2}}\frac{1}{\sqrt{\mathbf{q}^2+m^2}} \times\frac{1}{\sqrt{\mathbf{k}'^2+m^2}}\frac{1}{\sqrt{(\mathbf{k}'-\mathbf{q})^2+\mu^2}}.$$

In coordinate space, the wave equation becomes

$$\psi_{JM}(\mathbf{r}) = \int d^3\mathbf{r}' G_0(\mathbf{r}-\mathbf{r}',\sqrt{s})\int d^3\mathbf{z}\tilde{V}(\mathbf{r}',-\mathbf{z})\psi_{JM}(\mathbf{z}),$$

where $\psi_{JM}(\mathbf{r})$ and $\tilde{V}(\mathbf{r}',-\mathbf{z})$ are the Fourier transforms of the momentum-space two-particle wave function and effective potential, respectively. The free Green's function is given in Eq. (8). Performing the angular integral, the free Green's function reads

$$G_0(\mathbf{r},\sqrt{s}) = \frac{1}{2ir}\int_{-\infty}^{\infty}\frac{qdq}{(2\pi)^2}\frac{e^{iqr}-e^{-iqr}}{\sqrt{s}-2\sqrt{q^2+m^2}}, \quad \text{(A2)}$$

which has the following singularities in the complex q plane: two poles on the real axis, $q=\pm k$, and two branch cuts on the imaginary axis $\pm[im, i\infty]$, see Fig. 6. We choose the contour C_1+C_2 to include the pole at $q=k$ and circle around the cut $[im, i\infty]$ on the upper half-plane for first term with factor e^{ikr} and choose the contour C_1+C_3 to include the pole at $q=-k$ and circle around the cut $[-im,-i\infty]$ on the lower half-plane for the second term with factor e^{-ikr}, as shown in Fig. 6. The contour integral leads to

$$G_0(\mathbf{r},\sqrt{s}) = -\frac{\sqrt{s}}{2}\frac{e^{ikr}}{4\pi r}-\frac{1}{r}\int_m^{\infty}\frac{\rho d\rho}{(2\pi)^2}\sqrt{\rho^2-m^2}\frac{e^{-\rho r}}{k^2+\rho^2},$$

where $k=\frac{1}{2}\sqrt{s-4m^2}$ is the momentum of either particle in the rest frame of the two-particle system. The first term on the right-hand side comes from the poles at $q=\pm k$ and is proportional to the usual nonrelativistic Green's function which oscillates over the path of propagation. The second term comes from the contribution of the discontinuity crossing the branch cuts at $\pm[im, i\infty]$—it decays exponentially over the propagation. Expanding $\sqrt{\rho^2-m^2}=\rho(1-\mathcal{O}(\frac{m^2}{\rho^2}))$, at large separations, the free Green's function may be approximated by

$$G_0(\mathbf{r};\sqrt{s}) \approx -\frac{\sqrt{s}}{2}\frac{1}{4\pi r}\left[e^{ikr}+\frac{2}{\pi}\frac{e^{-mr}}{r\sqrt{s}}\right], \quad \text{(A3)}$$

and therefore the exponential decaying term can be dropped in the limit $r \gg m^{-1}$.

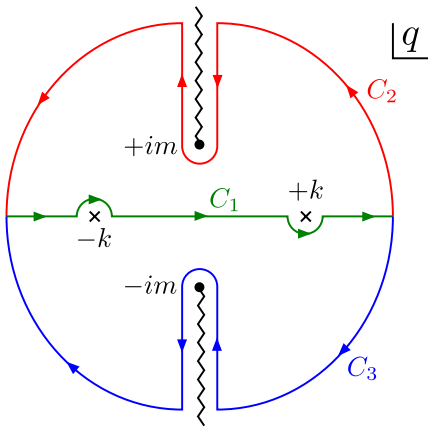

FIG. 6 (color online). Integration contours and singularities of the free Green's function in Eq. (A2) on the complex q plane.

APPENDIX B: EXPANSION OF GREEN'S FUNCTION AND REGULARIZATION OF EXPANSION COEFFICIENTS

We start from the expansion of the Green's function

$$\frac{1}{L^3}\sum_{\mathbf{q}\in\mathbf{P_Q}}\frac{e^{i\mathbf{q}\cdot\mathbf{r}}}{k^2-\mathbf{q}^2} = \frac{k}{4\pi}n_0(kr)-\sum_{jm_j}g^{(\mathbf{Q})}_{jm_j}(k)j_j(kr)Y_{jm_j}(\hat{\mathbf{r}}),$$

where the summation of $\mathbf{q}$ runs over $\mathbf{P_Q}=\{\mathbf{q}\in\mathbb{R}^3|\mathbf{q}=\frac{2\pi}{L}\mathbf{n}+\mathbf{Q}, \text{for } \mathbf{n}\in\mathbb{Z}^3\}$. The expansion coefficients are given by [8]

$$g^{(\mathbf{Q})}_{jm_j}(k) = \frac{4\pi}{L^3}\sum_{\mathbf{q}\in\mathbf{P_Q}}i^j\frac{q^j}{k^j}\frac{Y^*_{jm_j}(\hat{\mathbf{q}})}{\mathbf{q}^2-k^2}-\frac{\delta_{j0}\delta_{m_j0}}{\sqrt{4\pi}}\frac{1}{r}\Big|_{r\to 0}. \quad \text{(B1)}$$

Note that the definition of $n_j(x)$ in this work differs from the definition in [8] by an overall negative sign.

Using the identities

$$j_j(k|\mathbf{r}-\mathbf{r}'|)Y_{jm_j}(\widehat{\mathbf{r}-\mathbf{r}'}) \overset{r'<r}{=} \sqrt{4\pi}\sum_{\substack{lm_l\\ l'm_{l'}}}i^{l-l'-j}j_l(kr)j_{l'}(kr')Y_{lm_l}(\hat{\mathbf{r}})Y^*_{l'm_{l'}}(\hat{\mathbf{r}}') \times\sqrt{\tfrac{(2j+1)(2l'+1)}{2l+1}}\langle jm_j;l'm_{l'}|lm_l\rangle\langle j0;l'0|l0\rangle,$$

and

$$\frac{k}{4\pi} n_0(k|\mathbf{r}-\mathbf{r}'|) \overset{r'\leq r}{=} k\sum_{lm_l} n_l(kr) j_l(kr') Y_{lm_l}(\hat{\mathbf{r}}) Y^*_{lm_l}(\hat{\mathbf{r}}'),$$

we also have

$$\frac{1}{L^3}\sum_{\mathbf{q}\in\mathbf{P}_\mathbf{Q}} \frac{e^{i\mathbf{q}\cdot(\mathbf{r}-\mathbf{r}')}}{k^2-\mathbf{q}^2} \overset{r'\leq r}{=} \sum_{\substack{lm_l \\ l'm_{l'}}} [\delta_{l'm'_{l'},lm_l} n_l(kr) - \mathcal{M}^{(\mathbf{Q})}_{l'm'_{l'},lm_l}(k) j_l(kr)],\, k j_{l'}(kr') Y_{lm_l}(\hat{\mathbf{r}}) Y^*_{l'm_{l'}}(\hat{\mathbf{r}}'), \tag{B2}$$

with

$$\mathcal{M}^{(\mathbf{Q})}_{l'm'_{l'},lm_l}(k) = \sum_{jm_j} i^{l-l'-j} \frac{\sqrt{4\pi}}{k} g^{(\mathbf{Q})}_{jm_j}(k) \sqrt{\tfrac{(2j+1)(2l'+1)}{2l+1}} \langle jm_j; l'm_{l'}|lm_l\rangle \langle j0; l'0|l0\rangle. \tag{B3}$$

If $\mathbf{Q}$ is identified with $\frac{1}{2\gamma}\mathbf{P}$ for two-equal-mass-particle scattering, the generalization to two-unequal-mass-particle scattering leads to $\frac{1}{2\gamma}\mathbf{P}(1+\frac{m_1^2-m_2^2}{E^2})$ [33,34], these expressions are the same as those presented in [9], and the regularization procedure outlined therein can be followed. Once the Lorentz contraction is considered (substitution of box volume L^3 and momentum $\frac{2\pi}{L}\mathbf{n}$, $\mathbf{n}\in\mathbb{Z}^3$ by γL^3 and $\frac{2\pi}{L}\gamma^{-1}\mathbf{n}$ respectively), the function $g^{(\mathbf{Q})}_{jm_j}(k)$ is related to the zeta function defined in Eq. (93) of [9] by

$$g^{(\mathbf{Q})}_{jm_j}(k) = \frac{1}{\pi}\frac{1}{\gamma L}\frac{i^j}{(\frac{kL}{2\pi})^j} Z^{\mathbf{d}*}_{jm_j}\left(1, \frac{kL}{2\pi}\right). \tag{B4}$$

[1] C. Michael, Nucl. Phys. **B259**, 58 (1985).
[2] M. Luscher and U. Wolff, Nucl. Phys. **B339**, 222 (1990).
[3] B. Blossier, M. Della Morte, G. von Hippel, T. Mendes, and R. Sommer, J. High Energy Phys. 04 (2009) 094.
[4] J. J. Dudek, R. G. Edwards, M. J. Peardon, D. G. Richards, and C. E. Thomas (Hadron Spectrum Collaboration), Phys. Rev. D **82**, 034508 (2010).
[5] R. G. Edwards, J. J. Dudek, D. G. Richards, and S. J. Wallace, Phys. Rev. D **84**, 074508 (2011).
[6] J. J. Dudek, R. G. Edwards, and C. E. Thomas (Hadron Spectrum Collaboration), Phys. Rev. D **86**, 034031 (2012).
[7] L. Maiani and M. Testa, Phys. Lett. B **245**, 585 (1990).
[8] M. Lüscher, Nucl. Phys. **B354**, 531 (1991).
[9] K. Rummukainen and S. Gottlieb, Nucl. Phys. **B450**, 397 (1995).
[10] C.-J. D. Lin, G. Martinelli, C. T. Sachrajda, and M. Testa, Nucl. Phys. **B619**, 467 (2001).
[11] N. H. Christ, C. Kim, and T. Yamazaki, Phys. Rev. D **72**, 114506 (2005).
[12] V. Bernard, Ulf-G. Meißner, and A. Rusetsky, Nucl. Phys. **B788**, 1 (2008).
[13] V. Bernard, M. Lage, Ulf-G. Meißner, and A. Rusetsky, J. High Energy Phys. 08 (2008) 024.
[14] S. He, X. Feng, and C. Liu, J. High Energy Phys. 07 (2005) 011.
[15] M. Döring, Ulf-G. Meißner, E. Oset, and A. Rusetsky, Eur. Phys. J. A **47**, 139 (2011).
[16] S. Aoki, N. Ishii, T. Doi, T. Hatsuda, Y. Ikeda, T. Inoue, K. Murano, H. Nemura, and K. Sasaki (HAL QCD Collaboration), Proc. Jpn. Acad. Ser. B **87**, 509 (2011).
[17] R. A. Briceno and Z. Davoudi, arXiv:1204.1110.
[18] M. T. Hansen and S. R. Sharpe, Phys. Rev. D **86**, 016007 (2012).
[19] S. Aoki *et al.* (*CP*-PACS Collaboration), Phys. Rev. D **76**, 094506 (2007).
[20] K. Sasaki, and N. Ishizuka, Phys. Rev. D **78**, 014511 (2008).
[21] X. Feng, K. Jansen, and D. B. Renner, Phys. Rev. D **83**, 094505 (2011).
[22] J. J. Dudek, R. G. Edwards, M. J. Peardon, D. G. Richards, and C. E. Thomas (Hadron Spectrum Collaboration), Phys. Rev. D **83**, 071504 (2011).
[23] S. R. Beane, E. Chang, W. Detmold, H. W. Lin, T. C. Luu, K. Orginos, A. Parreño, M. J. Savage, A. Torok, and A. Walker-Loud (NPLQCD Collaboration), Phys. Rev. D **85**, 034505 (2012).
[24] C. B. Lang, D. Mohler, S. Prelovsek, and M. Vidmar, Phys. Rev. D **84**, 054503 (2011).
[25] S. Aoki *et al.* (CS Collaboration), Phys. Rev. D **84**, 094505 (2011)
[26] S. Glazek, A. Harindranath, S. Pinsky, J. Shigemitsu, and K. Wilson, Phys. Rev. D **47**, 1599 (1993).
[27] B. L. G. Bakker, M. van Iersel, and F. Pijlman, Few-Body Syst. **33**, 27 (2003).
[28] P. A. M. Dirac, Rev. Mod. Phys. **21**, 392 (1949).
[29] C. E. Thomas, R. G. Edwards, and J. J. Dudek, Phys. Rev. D **85**, 014507 (2012).
[30] A. M. Torres, M. Bayar, D. Jido, and E. Oset, Phys. Rev. C **86**, 055201 (2012).
[31] J. L. Basdevant and E. L. Berger, Phys. Rev. D **16**, 657 (1977).
[32] J. J. Dudek, R. G. Edwards, and C. E. Thomas, Phys. Rev. D **87**, 034505 (2013).
[33] Z. Fu, Phys. Rev. D **85**, 014506 (2012).
[34] L. Leskovec and S. Prelovsek, Phys. Rev. D **85**, 114507 (2012).